DOI: https://doi.org/10.4038/sljp.v24i2.8133

INSTITUTE OF PHYSICS – SRI LANKA

Review Article

Borophene as an anode material for metal-ion batteries

W. A. N. L. Perera, W. W. P. De Silva*

Department of Physics, University of Sri Jayewardenepura, Nugegoda, Sri Lanka

Abstract

Borophene is a novel 2D material whose history goes back only as far as the year 2015. Borophene is one atom thick 2D boron sheet which depict excellent optical, electronic, metallic, semiconducting, high mechanical anisotropic, and photothermal properties. Also, due to borophene's high mechanical strength, high specific capacity, and low diffusion barrier it poses as an ideal candidate as an anode material for metal metal-ion batteries. This is the avenue of interest of this review paper, where we intend to discuss the existing theoretical and experimental basis of various polymorphic structures of Borophene, as anode materials for metal-ion batteries.

Keywords: metal-ion batteries, borophene, boron, polymorphs

* Corresponding author: wasanthidesilva@sjp.ac.lk

1. INTRODUCTION

Boron is an element located at the boundary, separating metals and the non-metals of the periodic table, which inherit excellent electronic, optical, mechanical, semiconducting, metallic, photoacoustic, and photothermal properties. Also, due to the special characteristics of the B-B bond there are many innate polymorphic phases of bulk and monolayer of boron. The monolayer of boron is known as borophene, which is similar to graphene. The $2-Pmmn$, striped β_{12} χ_3, and honeycomb phases are the most prominent borophene polymorphic phases. These phases were successfully created by the epitaxial growth of boron atoms on silver surface in the presence of an ultra-high vacuum[1]. The synthetic atomic structures of monolayers vastly depend on the constituent element, processing conditions, and growth substrates. Borophene exhibits distinct physical and chemical characteristics. One example is the 2-Pmmn phase of borophene, which displays a buckled configuration where neighboring rows of boron atoms form corrugated patterns along the zigzag orientation. In the perpendicular in-plane direction (referred to as the armchair direction), the atomic arrangement remains flat and devoid of corrugations[2]. The relative energy assessment between bulk boron and a single layer of boron, known as borophene, hinges on multiple factors such as the crystal structure, bonding interactions, and external circumstances. The energy hierarchy may fluctuate depending on the particular configurations and patterns in which boron is arranged.

Under specific conditions, it is conceivable for monolayer borophene to exhibit a lower energy per atom in comparison to bulk boron. This could be attributed to variances in bonding, coordination, and the surface-related phenomena that emerge in low-dimensional systems such as monolayers. This can be overcome by using a substrate which can suppress the nucleation barrier of the bulk boron state and tempt to form a 2D layer[3]. The theoretical evidence indicates that the stability of borophene depends significantly on factors such as the concentration of hexagonal boron vacancies (denoted as x), the influence of the substrate, and chemical alterations[2]. The top-down, and bottom-up methods are used to fabricate borophene[4]. High speed transportation of carriers is predicted for the planar allotropes of borophene, which makes it an ideal candidate for electronic devices[5,6]. Borophen's bandgap can be regulated through the allotrope's crystallographic preparation[5,7]. Thus, one has the ability to choose between Dirac type no band gap state (similar to graphene) or parabolic type band gap state which depicts vast semiconductor characteristics[5]. This represents a significant advancement over its predecessor, as the previous approach required

the use of nano ribbons to induce a band gap in graphene. For instance, Alkali metals inserted on borophene vastly increase its binding energy and hydrogen storage capacities, which surpasses that of graphene.

Currently, batteries hold a pivotal position in advancing the most effective and adaptable energy storage technology during the ongoing worldwide shift from fossil fuels to renewable energies, facilitating emissions-free transportation [8]. Because of their portability and ability to be reused, rechargeable batteries have gained significant interest as a result of the quick growth of mobile devices and electric vehicles. The result of this electronic revolution was the development of metal-ion batteries with high energy and power densities, due to this, Lithium-ion batteries were developed and have been optimized throughout the past decades[9]. In the realm of battery technology, lithium-ion batteries possess an unparalleled blend of elevated energy and power densities, rendering them the preferred choice for applications like hybrid and all-electric vehicles, power tools, and specific portable electronics. With electric vehicles displacing conventional gasoline-powered transportation, lithium-ion batteries are poised to considerably diminish greenhouse gas emissions[10]. Additionally, due to their remarkable energy efficiency, these batteries can serve a variety of functions within power grids, such as enhancing the quality of energy harnessed from renewable sources like solar, wind, and geothermal. Such contributions from lithium-ion batteries hold the potential to substantially bolster the establishment of a sustainable energy economy. The limited number of lithium resources and continuous increase in cost of material had put a huge price for lithium production. Hence, there is an increase interest of replacing lithium ion with its' counter paths such as potassium-ion and sodium-ion due to their low production cost. In light of their relative abundance, favorable environmental compatibility, and greater charge densities, several Alkaline Earth Metals, including magnesium-ion, and calcium-ion, have been suggested as viable substitutes for lithium-ion.[9]. Graphite is the prevailing anode material in metal-ion batteries, and has many desirable characteristics, which makes it suitable to use as an electrode material. The low manufacturing cost, cyclic durability, and high Coulombic efficiency are the plus points of graphite's utility as an anode material[1], while its low power density[11] and low theoretical specific capacity[1] probes as the downsides for this material. Thus, the search for a replacement for the electrode material shifted from bulk materials to 2D layers due to the latter's superior qualities[1]. Graphene, the first monolayer to be discovered showed many favorable properties as a potential anode material, but also it possessed many drawbacks as

well[3,11,12]. Borophene is a light weight metallic monolayer of boron[12], well known for its very high theoretical specific capacity which can exceeds $1000\ \mathrm{mAhg^{-1}}$ and for very low theoretical diffusion barriers less than $0.7\ \mathrm{eV}$ for most of its phases with Lithium ion[3]. In other words, borophene may deliver high power density together with high energy density. Also, borophene inherit a good electrical conductivity[11,13], and high surface activity[5]. Borophene is the best material to use as a metal-ion battery anode because of its quick diffusion rate, thermal stability, and outstanding metallic and electrical characteristics. [12]. This paper mainly focuses on four different phases of borophene, and their potential as anode materials for metal-ion batteries.

2. DIFFERENT PHASES OF BOROPHENE AS ANODE MATERIAL FOR METAL-ION BATTERIES

2.1 Flat structure as anode material in metal-ion batteries

Computational Research has been conducted on four different flat borophene structures as anode material for lithium, sodium, magnesium and aluminum ion batteries. The precise proportion between the hexagonal vacancies and triangular units in these flat formations varies on the synthesis method, substrate type, and other experimental parameters[1]. Thus, this ratio could be used to identify polymorphic structures. Let us name these four structures as B1, B2, B3, and B4 for simplicity as shown in figure 1, and only the first two structures were synthesized experimentally while the latter were predicted through theoretical computations (see Figure 1). All DFT and first principal calculations were done on the supercell structures of B1, B2, B3, and B4, which contains 75, 80, 90, 128 boron atoms respectively. It is important to know that more negative the metal-ion adsorption is on a substrate, more suitable it is as an anode material. It was found that the hexagonal hollow sites generate the highest binding energy for all known borophene films with various adatoms[1]. The adsorption energies with different metal-ions for relevant flat borophene structures are listed in Table 1[1]. The negative adsorption energies indicate exothermic formation. The average adsorption energies were calculated by gradually increasing the relevant metal-ion coverage, and it was found that average aluminum adsorption of these sheets were endothermic, which makes them unsuitable for aluminum storage (see Figure 2)[1]. Lithium atoms were bounded more strongly than sodium atoms and sodium atoms in turn were bounded more strongly than the magnesium atoms. The open circuit voltage (OCV) remained positive for all the phases under whole range of adsorption values

indicating all the flat Borophene sheets are ideal candidates to be anode materials for Li, Mg and Na-ion batteries (see Figure 3)[1].

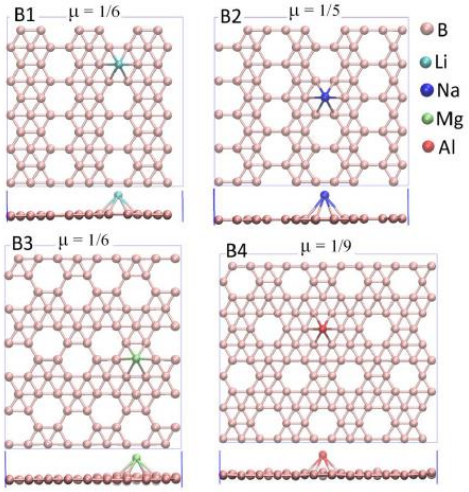

Figure 1 - Four different borophene sheets [1]

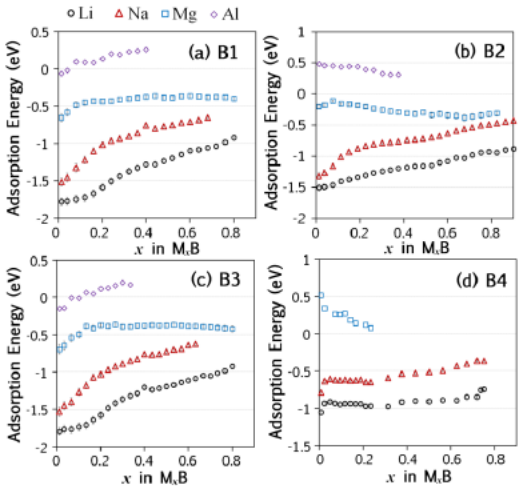

Figure 2 – Average adsorption energies for flat borophene sheets [1]

The variation of OCV was relatively small for the whole range of coverage values for Mg. The highest OCV was shown by Li-ion batteries, then by, Na-ion batteries and finally, Mg-ion batteries. The maximum charge capacities of each Borophene metal-ion along with varying hole densities are depicted in Table 2[1]. It was found that the flat borophene films were stable at high temperatures and after the full removal of adatoms[1]. The Figure 4 shows the diffusion barrier piercing the thickness of the sheet and extending along the armchair, zigzag, and diagonal lines. It was found that the diffusion is more favorable in the zigzag direction. The diffusion barrier of Li, and Na on B1 Borophene phase is in close agreement with the theoretical DFT values. The diffusion barrier values for B1 borophene sheet for Li, Na, and Mg was found to be 0.69 eV, 0.34 eV, and 0.97 eV respectively.

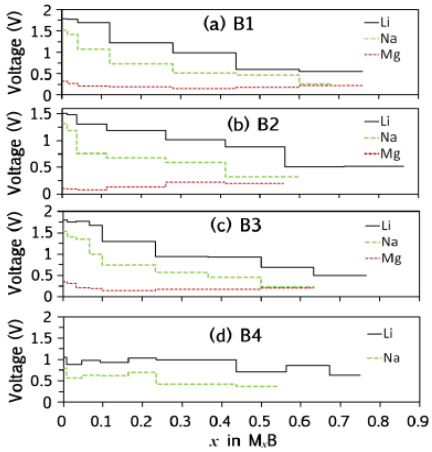

Figure 3 - OCV for flat borophene structures with various Metal-ions [1]

Table 1 - Adsorption energies for flat Borophene structures with various metal-ions [1]

Adsorption Energy (eV)				
Structure	Li	Na	Mg	Al
B1	-1.779	-1.51	-0.652	-0.0622
B2	-1.505	-1.318	-0.199	0.48
B3	-1.795	-1.53	-0.696	-0.144

Table 2 - Metal-ion capacities for flat Borophene structures [1]

Structure	Hexagonal Hole Density	Charge Capacity (mAh/g)		
		Li	Na	Mg
Buckled	0	1720	1380	1960
B4	1/9	1840	1340	-------
B1	1/6	1880	1640	2480
B3	1/6	1980	1550	2330
B2	1/5	2040	1480	2400

2.2 β_{12} Borophene as anode material for metal-ion batteries

The relaxed geometric structure of β_{12} borophene exhibits rectangular vacancy sites (see Figure 4)[13]. The ratio between the vacancy sites and Boron sites is $1:5$. The equilibrium lattice parameters are $a = 2.926$ Å and $b = 5.068$ Å [13]. The band structure contains two bands crossing the fermi level, which indicates metallic nature (see Figure 5)[13], and it was discovered from the predicted density of states that the P-orbitals largely control the metallic nature (see Figure 5). Also, this remains true for Li/Na intercalated states, thus making β_{12} borophene a suitable electrode material for battery. The negative adsorption energy indicates that the material favors metal-ion adsorption over forming a metal cluster. There are four meta-stable adsorption sites namely, $S_\beta 1$, $S_\beta 2$, $S_\beta 4$, and $S_\beta 11$ (see Figure 6)[13] and the adsorption energies of Na and Li at those sites are listed in Table 3[13]. The badger charge analysis and electronic structure calculations depicted that Li and Na transfer ~ 0.86 e and ~ 0.82 e respectively to β_{12} borophene[13]. In order to evaluate the diffusion barrier of the monolayer sheet, three distinct paths, P1, P2, and P3, with excellent structural symmetry between the adjacent stable adsorption sites, were taken into consideration. These pathways along with corresponding diffusion barrier profiles are shown in Figure 8 and Figure 9[13]. The P3 path shows the highest diffusion barrier, while the highest and lowest diffusion barrier voltages for the sheet were 0.66 eV and 0.33 eV respectively. The climbing-image

nudged elastic band (NEB) approach was used to achieve these results[13]. The average adsorption energy was calculated by increasing the Na/Li atoms layer wise, and the respective energies for each layer was reported[13]. The first layer of adatoms were absorbed above the $S_\beta 1$, while the second layer was absorbed at $S_\beta 2$, $S_\beta 4$, and $S_\beta 11$ due to the close relationship between their adsorption energies. The average adsorption energy for the first layer was found to be -1.216 eV for Li and -0.858 eV for Na, while for the second layer at the $S_\beta 11$ site the average adsorption values were -0.121 eV for Li and -0.062 eV for Na[13]. Higher layers were deemed to be unfavorable due to their positive adsorption energies[13]. The specific capacity for both Li and Na were found to be 1984 mAhg^{-1}[13]. Also, it is interesting to know that the addition of adatoms only alter the lattice constants slightly. The average OCV for Li decreased from 1.26 V to 0.61 V with the increase of adatoms, while for Na the average OCV variation was from 0.88 V to 0.42 V.

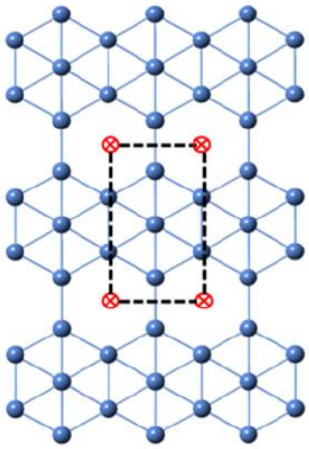

Figure 4 - Relaxed geometry [14]

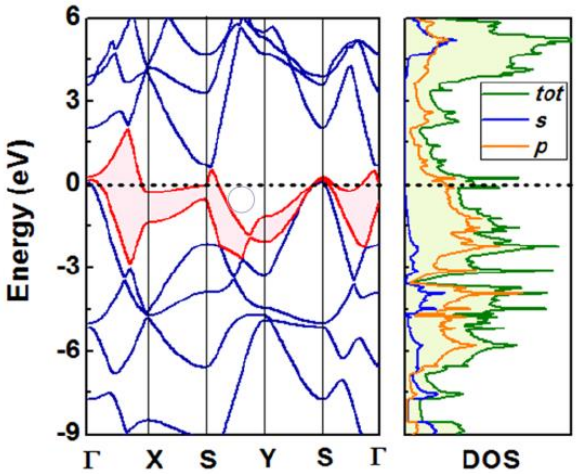

Figure 5 - Band and DOS profiles [14]

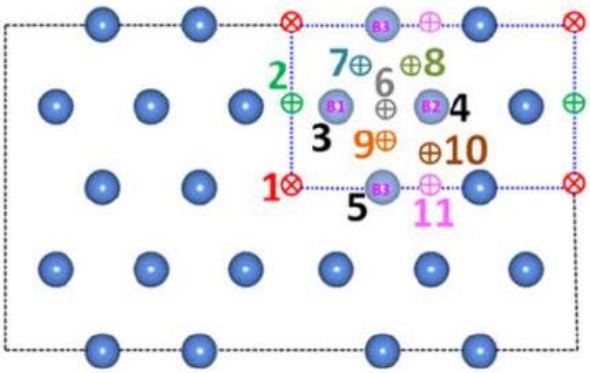

Figure 6 - Preferable adsorption sites [14]

Table 3 - Adsorption energy [14]

	$S_\beta 1$ (eV)	$S_\beta 2$ (eV)	$S_\beta 3$ (eV)	$S_\beta 11$ (eV)
β_{12}-B +Li	-1.766	-1.088	-1.027	-1.046
β_{12}-B +Na	-1.487	-1.163	-0.987	-1.027

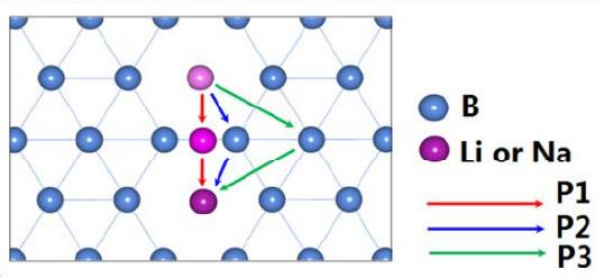

Figure 7 - Diffusion pathways [14]

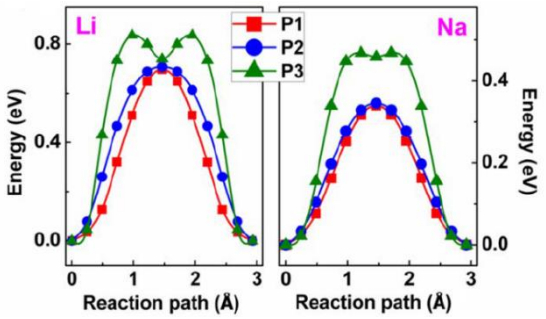

Figure 8 - Diffusion profile [14]

2.3 χ_3 Borophene as anode material for metal-ion batteries

The relaxed geometric structure of χ_3 borophene exhibits rhombic vacancy sites (see Figure 9). The ratio of vacant sites to boron sites is $1:4$. The equilibrium lattice parameters are $a = b = 4.490$ Å with a 38.181° rhombic cell angle[13]. The band structure and the DOS yield the same conclusion as the previously discussed β_{12} phase (see Figure 10)[13]. Thus, making χ_3 Borophene a suitable for battery electrode material. There are two meta-stable adsorption sites namely, $S_\chi 1$ and $S_\chi 2$ (see Figure 11)[13] and the adsorption energies of Na and Li at those sites are listed in Table 4. Thus, the most preferred adsorption site is above the vacancy site as depicted in figure 11. The badger charge analysis and electronic structure calculations depicted that Li and Na transfer ~ 0.86 e and ~ 0.82 e respectively to χ_3 Borophene. To evaluate the diffusion barrier of the monolayer sheet, three distinct paths, P1, P2, and P3 (see Figure 12), with excellent structural symmetry between the nearby stable adsorption sites, were taken into consideration. [13]. These pathways along with corresponding diffusion barrier profiles are provided by Figure 12 and Figure 13. The P3 path shows the highest diffusion barrier, while the highest and lowest diffusion barrier voltages for the sheet were 0.60 eV and 0.34 eV respectively. These values were obtained by using the climbing-image nudged elastic band (NEB) method[13]. The average

adsorption energy was calculated by increasing the Na/Li atoms layer in a single layer, since of χ_3 can absorb only a single layer. Thus, the maximum adsorption number is 8 for the $2 \times 2 \times 1$ supercell of χ_3 borophene. The specific capacity for both Li and Na were found to be $1240\ \text{mAhg}^{-1}$[13]. Also, it is interesting to know that the addition of adatoms only alter the lattice constants by 0.9 % for Li intercalation and 1.0 % for Na intercalation[13]. The average OCV for Li was found to be $1.09\ V$, while for Na it was found to be $0.78\ V$[13].

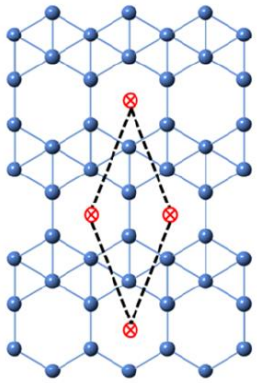

Figure 9 - Relaxed geometry [14]

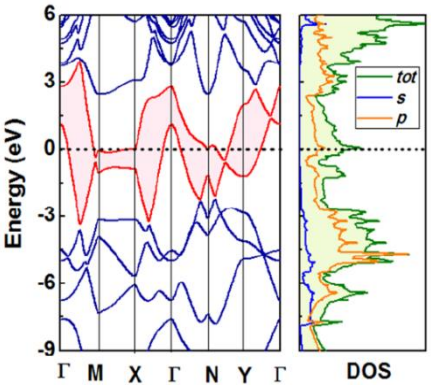

Figure 10 - Band and DOS profiles [14]

Table 4 - Adsorption energy [14]

	$S_\chi 1$ (eV)	$S_\chi 2$ (eV)
χ_3-B +Li	-1.433	-0.803
χ_3-B +Na	-1.230	-0.878

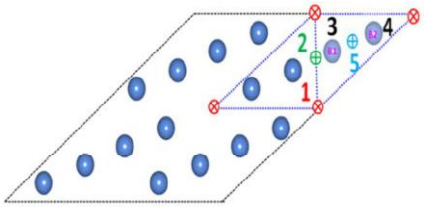

Figure 11 - Preferable adsorption sites [14]

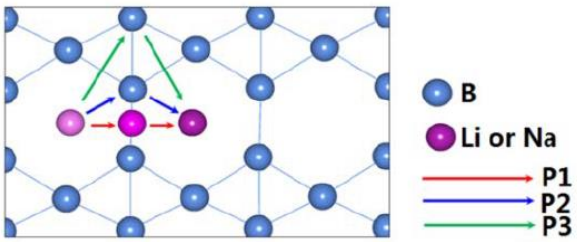

Figure 12 - Diffusion pathways [14]

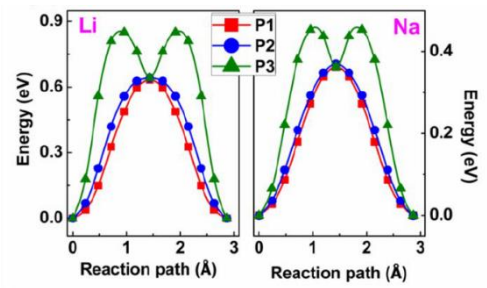

Figure 13 - Diffusion profile [14]

2.4 $Pmmn$ Borophene as anode material for metal-ion batteries

A 3×4 supercell with a primitive cell here contains 2 Boron atoms in two varying planes showing a bucking height of 0.881 Å along the z axis is considered in[11]. The optimized lattice constants are 2.886 Å and 1.619 Å along the corrugated and non-corrugated axis respectively (see Figure 14). Also, the B-B bond lengths along the two axes are 1.867 Å and 1.619 Å respectively[11]. A similar structure is used in [14], which utilize a supercell of 4×3 with a primitive cell of 2 Boron atoms. The optimized lattice parameters are 1.614 Å and 2.861 Å in the corrugated and the non-corrugated directions respectively (see Figure 15). The calculated B-B lengths for the above directions are 1.883 Å and 1.615 Å respectively[14].

Table 5 - Summarized results of [12,15]

	[11]	[14]
Li adsorption Binding/adsorption energy of the most preferred adsorption site Second most preferred site Third most preferred site Fourth most preferred site	$T_F - 1.12\ eV$ (See figure 17) $B_F - 1.11\ eV$ $T_R - 0.81\ eV$ $B_R - 0.79\ eV$	$T_C - 2.770\ eV$ (See figure 15)
Diffusion Barrier (Path – Barrier Voltage)	$T_F - B_R - T_F$ $- 325.1\ meV$ $T_F - B_F - T_F\ - 2.6\ meV$ (See figure 18)	x-1 $- 0.289\ eV$ x-2$-$ 0.267 eV y$-$ 0.007 eV (See figure 19)
Theoretical Specific Capacity	$Li_{0.75}B - 1860\ mAhg^{-1}$	$Li_{0.5}B - 1239\ mAhg^{-1}$
Open Circuit Voltage (OCV)	Not calculated	$Li_xB(0 \leq x \leq 0.25)$ $- 0.466V$ (See figure 20)

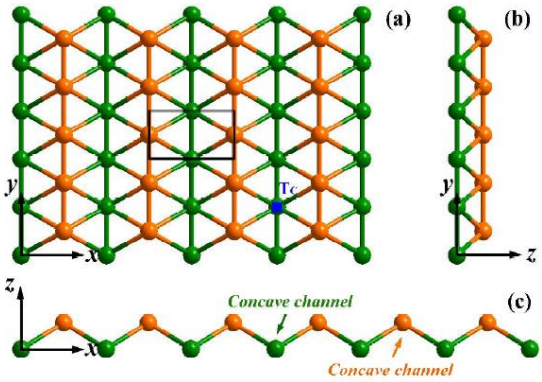

Figure 14 - The optimized structure [12]

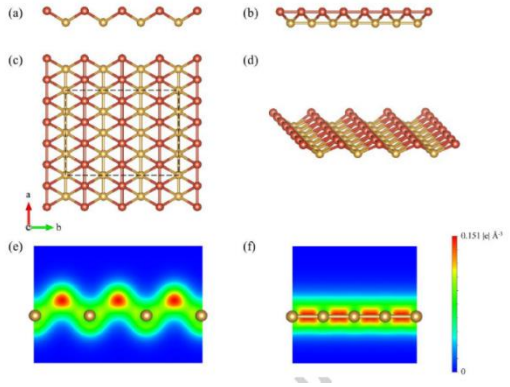

Figure 15 - The optimized structure 15]

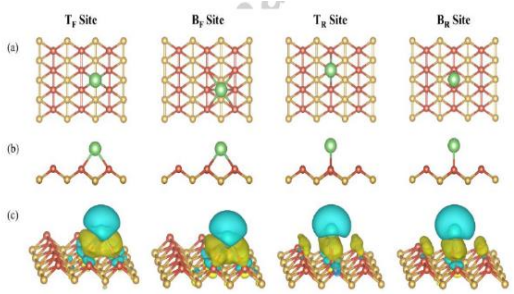

Figure 16 - Preferred Adsorption sites [15]

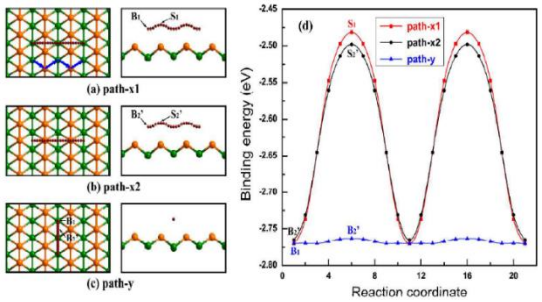

Figure 17 - Diffusion pathway and Binding energy profile [12]

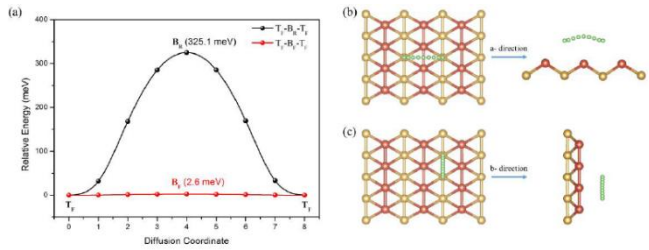

Figure 18 - Diffusion pathway and Binding energy profile [15]

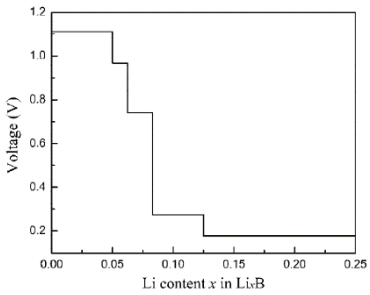

Figure 19 - OCV profile [12]

2.5 α/Honeycomb borophene as anode material for metal-ion batteries

The negative binding energies for the ML-h-Borophene (Monolayer hexagonal Borophene)-Li/Na systems show a robust adsorption process. In h-Borophene (Hexagonal Borophene), the barriers for Li and Na ion diffusion are calculated at 0.53 eV and 0.17 eV, respectively[15]. The anode's open-circuit voltages in LIB and NIB are 0.747 V and 0.355 V, respectively. H-Borophene's maximum theoretical storage capacity reaches 1860 $mAhg^{-1}$ for NIB and potentially as high as 5268 $mAhg^{-1}$ for LIB. This exceptional

capacity for LIB exceeds that of commercially utilized graphite ($372\ \mathrm{mAhg^{-1}}$) by over 14 times, establishing it as the material with the largest theoretical capacity among all known 2D materials.

All of the known types of borophene, non-buckled h-Borophene stands out due to its minimal molar mass per cell unit and the greatest concentration of hexagonal voids, which results in increased adsorption locations. These characteristics imply a potential for higher capacity compared to other borophene phases. As a result, comprehending the behavior of Li and Na ion adsorption and diffusion on h-Borophene is crucial in assessing its viability as an anode material.

On monolayer (ML) h-Borophene, Li and Na atoms prefer to inhabit the hollow site (H site). Lithium-ion batteries (LIB) with ML h-Borophene have a maximum storage capacity of $5268\ \mathrm{mAhg^{-1}}$, which is more than 14 times the capacity of LIB with graphite ($372\ \mathrm{mAhg^{-1}}$)[16]. Additionally, the theoretical specific capacity for sodium-ion batteries (NIB) using ML h-Borophene is notably 53 times higher at $1860\ \mathrm{mAhg^{-1}}$compared to graphite-based NIB at $35\ \mathrm{mAhg^{-1}}$[16,17]. The average open-circuit voltages (OCVs) projected for ML h-Borophene- $\mathrm{mAhg^{-1}}$A. 2×2 monolayer (ML) h-Borophene supercell is utilized, with a single Li/Na atom introduced for studying adsorption properties. The size of this supercell is sufficient to prevent interactions between neighboring Li/Na atoms in the periodic structure. The Figure 20 takes three separate high-symmetry adsorption sites into account: the hollow site (H site), which is positioned above the hexagon's center, the bridge site (B site), which is situated on the B-B bond, and the atom point site (T site), which is positioned on top of a B atom. In terms of total energy, the adsorption of a Li/Na atom onto the H site of the 2×2 ML h-Borophene supercell yields the most favorable result compared to adsorption on the H, B, and T sites.

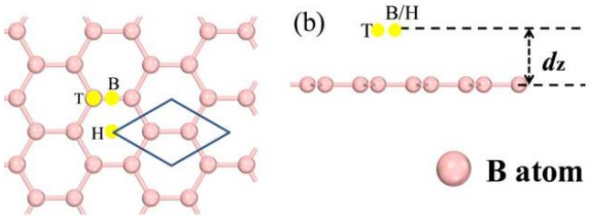

Figure 20 – Preferred adsorption sites [16]

Table 6 - Adsorption and Binding energies for Li [16]

	Adsorption Site		
	Hollow	Bridge	Top
Adsorption distance d_a (Å)	1.41	-	2.11
Total Energy E_t (eV)	-46.89	-	-46.33
Binding Energy E_b (eV $atom^{-1}$)	-1.06	-	-0.50
Charge Transfer (e^-)	0.84	-	0.88

Table 7- Adsorption and Binding energies for Na [16]

	Adsorption Site		
	Hollow	Bridge	Top
Adsorption distance d_a (Å)	1.99	2.30	2.41
Total Energy E_t (eV)	-45.90	45.72	-45.70
Binding Energy E_b (eV $atom^{-1}$)	-0.68	0.50	-0.48
Charge Transfer (e^-)	0.76	0.79	0.79

A stronger exothermic and spontaneous reaction between the Li/Na atom and ML h-Borophene occurs with a reduced binding energy of the adsorbed Li/Na atom. The binding energies (Eb) for Li and Na ions on the H site are -1.06 eVatom^{-1} and -0.68 eVatom^{-1}, respectively. The energy barrier for diffusion in the zigzag direction is 0.53 eV for Li ions and 0.17 eV for Na ions, with both having a pathway length of about 3.69 Å. In this direction, the energy profile indicates that the B site is the most energetically unfavorable state, surpassing the H site by approximately 0.53 eV and 0.17 eV [15]for Li and Na ions, respectively.

In contrast, the energy barrier for diffusion in the armchair direction is 0.54 eV for Li ions and 0.19 eV for Na ions, with corresponding pathway lengths around 5.90 Å. Here, the energy profile shows the B site as an intermediate state, again being energetically less favorable than the H site by about 0.53 eV and 0.17 eV for Li and Na ions, respectively. The T site is identified as the transition state, positioned higher in energy than the H site by approximately 0.54 eV and 0.19 eV for Li and Na ions, respectively[15].

Li/Na ions don't specifically depend on the diffusion path for the height of the diffusion barrier, however the zigzag direction often provides a shorter diffusion pathway than the

armchair direction. Furthermore, the density of the diffusion barrier (determined by the ratio of the number of diffusion barrier heights exceeding 0.5 eV for Li or 0.15 eV for Na to the corresponding pathway length) in the zigzag direction is lower than that in the armchair. The diffusion barrier height for the Li ion is greater compared to that of the Na ion, making its migration more challenging on the surface of ML h-Borophene. However, the diffusion barrier height for the Li ion on ML h-Borophene (0.53 eV) remains lower than those observed on ML β_{12} (0.66 eV) and X_3 (0.60 eV) Borophene[15].

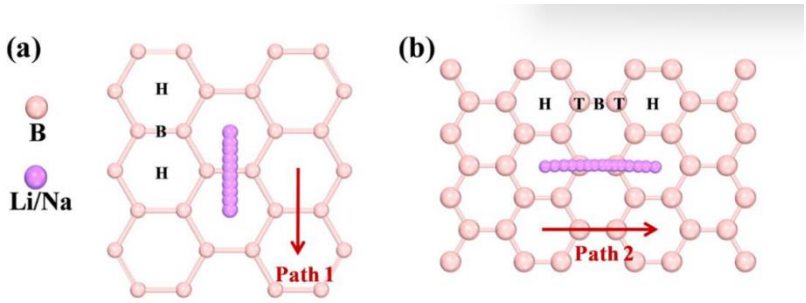

Figure 21(a) - Diffusion pathway in the zigzag direction [16]

Figure 21(b) - Diffusion pathway in the armchair direction [16]

The computed maximum theoretical storage capacity, denoted as C, is exceptionally elevated, reaching 5268 $mAhg^{-1}$for lithium-ion batteries (LIB)[18] and 1860 $mAhg^{-1}$ for sodium-ion batteries (NIB). Importantly, it's worth highlighting that ML h-Borophene' s maximum theoretical storage capacity for LIB as an electrode surpasses that of all previously reported 2D materials, signifying its remarkable capacity. The open-circuit voltages (OCVs) exhibit distinct values depending on the concentration for both lithium-ion batteries (LIB) and sodium-ion batteries (NIB). In the case of LIB, OCVs span from 1.06 V to 0.95 V in increments of 0.125, encompassing concentrations from 0 to 1.000. Additionally, OCVs for concentrations of 1.250, 1.750, 2.000, and 2.125 yield values of 0.50 V, 0.16 V, 0.09 V, and 0.03 V respectively. The overall average OCV for LIB is 0.747 V[15].

As for NIB, OCVs vary from 0.68 V to 0.04 V in steps of 0.125, encompassing concentrations from 0 to 0.75. The overall average OCV for NIB is 0.355 V. Monolayer (ML) h-Borophene possesses intrinsic metallic properties. A Dirac state is present at an energy level of 3.33 eV; however, this state is considerably distant from ML h-Borophene' s Fermi level. Consequently, this electronic state has no impact on the material's metallic characteristic[19,20].

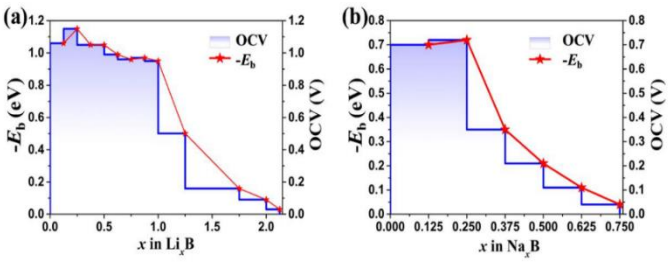

Figure 22 - OCV voltage variation [16]

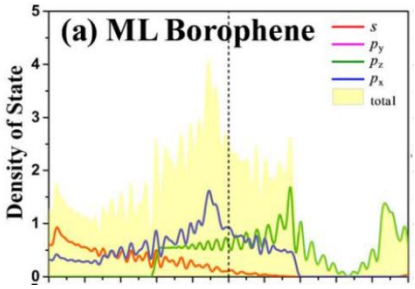

Figure 23 - Density of states of monolayer hexagonal Borophene [16]

3. SUMMARY

Flat borophene has many advantages over the β_{12}, χ_3, and $Pmmn$ phases. Namely, the maximum specific capacity achieved by Li-ion in flat borophene was $2040\ \text{mAhg}^{-1}$, while for the latter phases this value is lesser except for the honeycomb phase, $1984\ \text{mAhg}^{-1}$, $1240\ \text{mAhg}^{-1}$, $1860\ \text{mAhg}^{-1}$, and $5268\ \text{mAhg}^{-1}$ respectively. On the contrary, for Na-ion β_{12} has the highest capacity followed by honeycomb Borophene, flat Borophene and χ_3 phase. The relevant values are $1860\ \text{mAhg}^{-1}$,$1984\ \text{mAhg}^{-1}$, $1640\ \text{mAhg}^{-1}$, and $1240\ \text{mAhg}^{-1}$. The Li and Na-ion OCV are highest for the flat Borophene, then for the β_{12} phase, followed by honeycomb and χ_3 phases. The relevant values are $1.75\ \text{V}$, $1.09\ \text{V}$, $0.747\ \text{V}$, and $0.69\ \text{V}$ for Li-ion, and $1.5\ \text{V}$, $0.78\ \text{V}$, $0.355\ \text{V}$, and $0.34\ \text{V}$ for Na ion. The diffusion barrier is highest for the flat borophene followed by, β_{12}, χ_3, and phases for Li-ion. The respective values are $0.69\ \text{V}$, $0.66\ \text{V}$, $0.60\ \text{V}$, and $0.54\ \text{V}$ but for Na-ion both flat and χ_3 phase was found to have a barrier of $0.34\ \text{V}$, while for β_{12} phase the diffusion barrier was $0.33\ \text{V}$. The diffusion barrier for the honeycomb phase was a negligibly smaller value of $0.19\ \text{V}$ when compared with the values of its counter paths. The diffusion barrier for the $Pmmn$ phase was found to be lowest in the un-corrugated direction. A value of $0.007\ \text{V}$, which a minuscule when compared with its counter paths. Also, the OCV takes the value $0.466\ \text{V}$ for $Li_xB(0 \leq x \leq 0.25)$. Therefore, even though flat Borophene has a larger capacity and a high OCV when compared to the β_{12} and χ_3 phases, it has the highest diffusion barrier voltage, but the barrier voltages only vary slightly between these phases except for the $Pmmn$ phase and honeycomb phase. On the other hand, the honeycomb phase has the largest capacity with a OCV less than its' counter paths other than $Pmmn$, but it has a low diffusion barrier compared to the flat Borophene, β_{12} and χ_3 structures, Thus, it is safe to conclude that the honeycomb Borophene depict overall better performance as an anode material over the flat, β_{12}, χ_3, and $Pmmn$ phases of Borophene.

REFERENCES

1. Mortazavi B, Rahaman O, Ahzi S and Rabczuk T 2017 Flat borophene films as anode materials for Mg, Na or Li-ion batteries with ultra high capacities: A first-principles study *Appl Mater Today* **8** 60–7
2. Wang Z Q, Lü T Y, Wang H Q, Feng Y P and Zheng J C 2019 Review of borophene and its potential applications *Front Phys (Beijing)* **14**
3. Sengupta A 2022 First principles study of Li adsorption properties of a Borophene based hybrid 2D material B5Se *Applied Surface Science Advances* **8**
4. Xie Z, Meng X, Li X, Liang W, Huang W, Chen K, Chen J, Xing C, Qiu M, Zhang B, Nie G, Xie N, Yan X and Zhang H 2020 Two-Dimensional Borophene: Properties, Fabrication, and Promising Applications *Research* **2020** 1–23
5. Krowne C M and Sha X 2021 Atomic structural and electronic bandstructure calculations for borophene *Mater Res Express* **8**
6. Fiori G, Bonaccorso F, Iannaccone G, Palacios T, Neumaier D, Seabaugh A, Banerjee S K and Colombo L 2014 Electronics based on two-dimensional materials *Nat Nanotechnol* **9** 768–79
7. Wu X, Dai J, Zhao Y, Zhuo Z, Yang J and Zeng X C 2012 Two-dimensional boron monolayer sheets *ACS Nano* **6** 7443–53
8. Verma J and Kumar D 2021 Metal-ion batteries for electric vehicles: current state of the technology, issues and future perspectives *Nanoscale Adv* **3** 3384–94
9. Kasprzak G T and Durajski A P 2022 Two-dimensional B 2 C as a potential anode material for Mg-ion batteries with extremely high theoretical capacity *Sci Rep* **12**
10. Larcher D and Tarascon J M 2015 Towards greener and more sustainable batteries for electrical energy storage *Nat Chem* **7** 19–29
11. Zhang Y, Wu Z F, Gao P F, Zhang S L and Wen Y H 2016 Could Borophene Be Used as a Promising Anode Material for High-Performance Lithium Ion Battery? *ACS Appl Mater Interfaces* **8** 22175–81
12. Folorunso O, Hamam Y, Sadiku R, Ray S S and Adekoya G J 2021 Theoretical analysis of borophene for lithium ion electrode *Materials Today: Proceedings* vol 38 (Elsevier Ltd) pp 485–
13. Zhang X, Hu J, Cheng Y, Yang H Y, Yao Y and Yang S A *Borophene as an extremely high capacity electrode material for Li-ion and Na-ion batteries*
14. Jiang H R, Lu Z, Wu M C, Ciucci F and Zhao T S 2016 Borophene: A promising anode material offering high specific capacity and high rate capability for lithium-ion batteries *Nano Energy* **23** 97–104
15. Li J, Tritsaris G A, Zhang X, Shi B, Yang C, Liu S, Yang J, Xu L, Yang J, Pan F, Kaxiras E and Lu J 2020 Monolayer Honeycomb Borophene: A Promising Anode Material with a Record Capacity for Lithium-Ion and Sodium-Ion Batteries *J Electrochem Soc* **167** 090527
16. Slater M D, Kim D, Lee E and Johnson C S 2013 Sodium-ion batteries *Adv Funct Mater* **23** 947–58

17. Yabuuchi N, Kubota K, Dahbi M and Komaba S 2014 Research development on sodium-ion batteries *Chem Rev* **114** 11636–82

18. Nitta N, Wu F, Lee J T and Yushin G 2015 Li-ion battery materials: Present and future *Materials Today* **18** 252–64

19. Tarascon J-M and Armand M 2001 *Issues and challenges facing rechargeable lithium batteries*

20. Lu L, Han X, Li J, Hua J and Ouyang M 2013 A review on the key issues for lithium-ion battery management in electric vehicles *J Power Sources* **226** 272–88